Published in final edited form as:
J Vasc Surg. 2013 December ; 58(6): . doi:10.1016/j.jvs.2013.02.241.

Reduced hind limb ischemia-reperfusion injury in Toll-like receptor-4 mutant mice is associated with decreased neutrophil extracellular traps

Rahmi Oklu, MD, PhD[1,3], **Hassan Albadawi, MD**[2,3], **John E. Jones, M.D.**[2], **Hyung-Jin Yoo, MS**[2], and **Michael T. Watkins, MD, FACS**[2,*]

[1]Harvard Medical School, Massachusetts General Hospital, Division of Vascular Imaging and Intervention, Boston, MA

[2]Harvard Medical School, Massachusetts General Hospital, Division of Vascular and Endovascular Surgery, Boston, MA

Abstract

Objective—Ischemia-reperfusion (IR) injury is a significant problem in the management of patients with acute limb ischemia (ALI). Despite rapid restoration of blood flow following technically successful open and endovascular revascularization, complications secondary to IR injury continue to occur and limit clinical success. Our aim was to create a murine model of hind limb IR injury to examine the role of Toll-like receptor-4 (TLR4) and to determine whether inactive TLR4 led to a decrease in the detection of neutrophil extracellular traps (NETs), which is known to be highly thrombogenic and may mediate microvascular injury.

Methods—A calibrated tension tourniquet was applied to unilateral hind limb of wild type (WT) and TLR4 receptor mutant (TLR4m) mice for 1.5 hours to induce ischemia and then immediately removed to initiate reperfusion. At the end of 48 hours of reperfusion, mice were sacrificed and hind limb tissue as well as serum specimens were collected for analysis. Hematoxylin and eosin stained sections of hind limb skeletal muscle tissue were examined for fiber injury. For immunohistochemistry, mouse monoclonal anti-histone H2A/H2B/DNA complex antibody to detect NETs and rabbit polyclonal anti-myeloperoxidase (MPO) antibody were used to identify infiltrating cells containing MPO. Muscle ATP levels, nuclear NF-κB activity, IκBα, poly (ADP-ribose) polymerase (PARP) activity and iNOS expression were measured. Systemic levels of KC, MCP-1 and VEGF in the serum samples were also examined.

Results—IR injury in the hind limb of wild type mice demonstrated significant levels of muscle fiber injury, decreased energy substrates, increased NF-κB activation, decreased I-κBα levels, increased iNOS expression and increased PARP activity levels when compared to the TLR4 knockout mice samples. Additionally, there was marked decrease in the level of neutrophil and monocyte infiltration in the TLR4 mutant mice, which corresponded to similar levels of decreased NETs detection in the interstitial space and in microvascular thrombi. *In situ* nuclease treatment of wild-type tissue sections significantly diminished the level of NETs immunostaining

*Corresponding author, For all correspondence, please contact: Michael T. Watkins, MD, FACS, Massachusetts General Hospital, Division of Vascular and Endovascular Surgery, 15 Parkman St., Ste. 440, Boston, MA 02114, mtwatkins@partners.org.
[3]These authors contributed equally.

demonstrating the specificity of our antibody to detect NETs and suggesting a potential role for nuclease treatment in IR injury.

Conclusions—These results suggest a pivotal role for TLR4 in mediating hind limb IR injury and suggest that NETs may contribute to muscle fiber injury.

Introduction

The cornerstone for the treatment of acute limb ischemia is to rapidly restore blood flow to the limb in order to minimize ischemia-reperfusion (IR) injury, which occurs when blood is reintroduced into the oxygen-deprived limb. The mechanism of reperfusion injury is complex involving a vigorous inflammatory response to reflow in which the innate immune system plays a central role. IR injury is in part mediated by pro-inflammatory cytokines, endothelial cell activation, reactive oxygen species and neutrophil infiltration and activation. There is growing evidence linking the Toll-like receptor (TLR) family of proteins of the innate immune system, specifically TLR4, and the development of IR injury in myocardial infarction, stroke, intestinal ischemia, transplantation and sepsis.[26, 32–34] The role of TLR4 in IR has been largely derived from murine models deficient in the functional form of the TLR4 gene. Deficiency of TLR4 provides significant protection from tissue injury in hepatic transplant models, murine models of cardiac, cerebral and renal ischemia-reperfusion and hemorrhagic shock.[11, 26, 34, 35, 37]

Neutrophils play a key role in the inflammatory response raised against IR injury. Their accumulation into an inflamed site is directed by cytokines and, upon activation, neutrophils can release neutrophil extracellular traps (NETs), which are comprised of neutrophil genomic DNA studded with cytoplasmic granular proteins released into the extracellular matrix.[12] Although NETs were initially detected in infectious tissues such as appendicitis, shigellosis, fasciitis and pneumonia, they have also been detected in plasma and thrombus.[3, 4, 25] In infection, NETs seem to have a protective, antimicrobial effect. In thrombosis, however, NETs appear to have a deleterious effect by playing a role in clot formation directly by stimulating platelets via the TLR4 pathway.[3, 5, 13]

In this study, experiments were designed to test the hypothesis that TLR4 modulates skeletal muscle injury, inflammation and the production of NETs in response to IR. To test this hypothesis, murine hind limb IR injury was created in both wild type and TLR4 mutant mice. Several factors were examined to assess structural muscle damage (histologic examination), skeletal muscle energy metabolism (ATP) and, along with markers of inflammation (iNOS mRNA, Poly (ADP-ribose) polymerase (PARP) activity), expression of p65 NF-κB protein and the alpha subunit of the inhibitor of NF-κB protein I-κBα, systemic inflammation (serum cytokines) and angiogenesis (serum vascular endothelial growth factor (VEGF)). Lastly, the detection of NETs within the injured hind limb was examined using immunohistochemistry to determine whether the functional status of TLR4 was associated with the amount of NETs detected and the level of tissue injury.

Methods

Animal Protocols

Animal care and experimental procedures were in compliance with the “Principal of Laboratory Animal Care” (Guide for the Care and Use of Laboratory Animals, National Institutes of Health publication 86–23, 1985) and approved by the Institutional Review Committee. 8–12 weeks of age C3H/HeJ TLR4 mutants (TLR4m)[28] and wild type C3H/HeSnJ (Jackson Lab, Bar Harbor, ME) mice were housed in pathogen-free cages and were given free access to water and standard rodent chow. 1.5 hour of hind limb ischemia

followed by reperfusion was created as previously described.[8] After 48 hours of reperfusion, mice were sacrificed, hind limb tissue and serum specimens were collected. Hind limbs were either fixed for histologic analysis or immediately frozen in liquid nitrogen and stored at −80˚C for future analysis.

Histology and Immunohistochemistry

Muscle Injury—5-micron transverse sections of hind limb muscle tissue were stained with hemotoxylin and eosin (H&E) to visualize the morphology of the tissues. To determine muscle fiber injury in each of the hind limb specimens (WT, n=8; TLR4m, n=8), sixteen images from the H&E stained sections at 200X magnification of the anterior tibialis and gastrocnemius muscle groups were obtained using a light microscope following 48 hours of reperfusion. Each image was assigned a distinct number using SPOT Insight microscope camera software (Diagnostic Instruments, Sterling Heights, MI) and analyzed as previously described.[21] Muscle fiber injury was indicated by the presence of destroyed cell membrane, loss of nuclear morphology and loss of polygonal shape of the muscle fiber. The data was expressed as the percent of injured fibers from the total number of muscle fibers counted in each tissue sample, as previously described.[21]

Inflammatory Cell Infiltration—Since myeloperoxidase is produced by neutrophils and macrophages,[9, 31] tissue sections were immunostained for this protein (WT, n=8; TLR4m, n=8). Rabbit polyclonal anti-myeloperoxidase (MPO) (Abcam, Cambridge, MA) was used for detection at a concentration of 1 μg/mL. The secondary antibody, anti-rabbit IgG conjugated to horseradish peroxidase enzyme (Vector Labs, Burlingame, CA), was also used in the same concentration. Sections were developed using 3,3'-diaminobenzindine chromogen reagent solution (R&D Systems, MN, USA) according to the manufacturer's instructions. A Carl Zeiss microscope (100TV; Carl Zeiss Micro Imaging, USA) with a multi-band filter block was used to visualize the tissue sections. Images of these sections were taken using a Quantifire X1 digital camera (Optronics, Goleta, CA) and processed using Pictureframe (Optronics, Goleta, CA). For negative controls, the MPO antibody was omitted and substituted with 1 μg/mL dilution of the anti-rabbit IgG. Similar to the quantitation of the muscle fiber assay above, 20 images at 200X magnification for each hind limb muscle tissue sections immunostained for MPO were assigned a number using a random number generator. 16 of the 20 images from each hind limb tissue were uploaded using Adobe Photoshop software and a blinded reviewer then counted all MPO positive cells; the data are expressed as mean number of MPO positive cells/high power field (hpf; 200x) ± standard error for each group.

NETs detection—Hind limb tissue sections were developed using cyanine-3 tyramide signal amplification kit (Perkin Elmer, Boston, MA) according to the manufacturer's instructions (WT, n=8; TLR4m, n=8). The mouse monoclonal anti-histone H2A/H2B/DNA complex antibody (gift of Dr. Marc Monestier, Temple University, PA) and the anti-mouse IgG antibody (Vector Labs, Burlingame, CA) were used to detect NETs at 1 μg/mL dilution.[18] Sections for immunofluorescence were mounted using mounting medium (Vectashield; Vector Labs, Burlingame, CA) containing 4',6-diamidino-2-phenylindole (DAPI). As above, a Carl Zeiss microscope (100TV; Carl Zeiss Micro Imaging, USA) was used to image the immunofluorescent slides. For negative control, the NETs antibody was omitted and substituted with 1 μg/mL dilution of the anti-mouse IgG. To demonstrate the specificity of the mouse monoclonal anti-histone H2A/H2B/DNA complex antibody to detect NETs, a subset of tissue sections were initially treated with 10 units of DNase enzyme (New England Biolabs, MA, USA) for 30 min at 37°C. These sections were not treated with triton X-100 to minimize permeabilization.

Muscle Adenosine Triphosphate (ATP) Quantitation

200 mg of each frozen hind limb muscle tissue (WT, n=5; TLR4m, n=5) was homogenized on ice in 10% trichloroacetic acid using a polytron tissue disruptor. The supernatant from each sample was collected following centrifugation for 10 minutes, 10,000 xg at 4°C. Each sample was diluted using Dulbecco's modified phosphate buffered saline (DPBS with Ca++ and Mg++, pH=7.4). ATP levels (nmole per mg tissue) were measured using the ATPlite luminescence assay (PerkinElmer Life, Boston, MA) following the manufacturer's instructions.

NF-κB activity

Total nuclear protein extracts were prepared from fresh hind limb tissue (WT, n=5; TLR4m, n=5) using a nuclear extraction kit (Active Motif, Carlsbad, CA), following the manufacturer's instructions. Briefly, 200 mg of tissue was trimmed from the posterior calf muscle, rinsed in ice cold PBS and immediately homogenized in a hypotonic buffer supplemented with 1μl of a detergent mix and 1 μl/ml of 1M DTT. The homogenate was placed on ice for 30 minutes and centrifuged for 10 minutes at 850 xg, 4ºC. After re-suspending the pellet in a hypotonic buffer, 50 μl /ml of detergent was added for each milliliter of total volume and then mixed and centrifuged for 30 second at 14,000 xg. The supernatant was decanted and the pellet was re-suspended in a lysis buffer. Samples were rocked on ice for 30 minutes and centrifuged for 10 minutes at 14,000 xg at 4°C. The supernatant was collected and aliquots were stored at −80°C until analysis. The concentration of the proteins was determined using a bicinchoninic acid assay with bovine serum albumin (BSA) as the standard (Pierce Biotechnology, Rockford, IL), following manufacturer's instructions. To estimate NF-κB activation in the hind limb tissues, a Trans-AM™ NF-κB p65 Transcription Factor Assay Kit was used (Active Motif, Carlsbad, CA) following manufacturer's instructions. 20 μg of each of the nuclear protein samples were used in the assay. Results are presented as a mean OD 450 nm ±SEM.

IκBα expression and PARP activity

100 μg of total protein isolated from each hind-limb tissue (WT, n=5; TLR4m, n=5) was solubilized with equal volume of Laemmli sample buffer (0.25M Tris-HCl pH 6.8, 8% SDS, 40% glycerol, 0.4M DTT and 0.04% Bromophenol Blue) (BioRad, Hercules CA), boiled for 5 minutes and then loaded onto lanes in a 4–15% density gradient Tris-HCl polyacrylamide/ sodium dodecyl sulfate (SDS) gel. Samples were subjected to electrophoresis followed by electro-blotting transfer using a 0.22 μm nitrocellulose membrane (BioRad, Hercules, CA). The membranes were blocked (Western blot blocker, Sigma-Aldrich) for 1 hour at room temperature. To assess PARP activity, the membranes were incubated with monoclonal anti-poly-(ADP)-ribose antibody (1:2000 dilution, Tulip Biolabs, West Point, PA) that detect poly (ADP)-ribose-modified proteins in the muscle extracts. To determine the level of total and phosphorylated inhibitor of NFκB alpha subunit (IκBα), membranes were incubated with polyclonal rabbit anti-IκBα antibody or polyclonal rabbit anti phosphor-IκBα (pSer32) antibody (1:1000 dilution for both antibodies; Cell Signaling Technology, Danvers, MA, USA) for 1 hour at room temperature. Membranes were then probed with goat anti-mouse or goat anti-rabbit horseradish peroxidase conjugated IgG at 1:4000 dilution in blocking buffer for one hour at room temperature. After washing the membranes, they were developed using the enhanced chemiluminescence detection system (GE, Healthcare, Piscataway, NJ). The generated specific protein band integrated density values (IDV) were measured using the FluorChem HD2 Imager system (Cell Biosciences, Santa Clara, CA). The membranes were stripped and re-probed using anti-mouse α-tubulin IgG (Abcam, Cambridge, MA).

iNOS mRNA expression

Semi quantitative RT-PCR—Total RNA was isolated from hind-limb tissue (WT, n=5; TLR4m, n=5) after homogenization in Trizol Reagent (Invitrogen, Carlsbad, CA) followed by chloroform phase separation and 2-Propanol precipitation. Total RNA samples were purified by Qiagen silica gel membrane column (Qiagen, Valencia, CA). The concentration of total RNA was determined by measuring the absorption at 260 nm and the purity of the purified RNA was assessed by the ratio between the absorbance values at 260 nm and 280 nm. Equal amounts of total RNA were reverse transcribed using SuperScript First-Strand Synthesis System (Invitrogen, Carlsbad, CA) and Oligo (dT) primers. iNOS cDNA was amplified using platinum blue PCR super mix as follows: 94°C for 30 seconds, 55°C for 30 seconds and 72°C for 60 seconds for a total of 30 cycles. Primer pair sequences used for iNOS were previously described [30]. The following β-actin primers were used: 5'-CAGGTCATCACTATTGGCAACG-3' and 5'-CACAGAGTACTTGCGCTCAGGA-3' for 26 cycles. The reaction mix of each sample was subjected to 1.5% agarose electrophoreses in TAE buffer. Alpha Imager 1000 system (Alpha Innotech Corporation, San Leandro, CA) was used to calculate the bands integrated density values (IDV) after background correction. Data was normalized to β-actin bands densities.

Serum Cytokines and VEGF

Serum aliquots (WT, n=8; TLR4m, n=8) obtained following 48 hours of reperfusion were assayed for keratinocyte-derived cytokine (KC), monocyte chemoattractant protein-1 (MCP-1) and vascular endothelial growth factor (VEGF) using quantitative ELISA (R&D Systems, Minneapolis, MN) according to manufacturer's protocol.

Statistical analysis

Statistical analysis between two groups was performed with Instat (Graph pad, San Diego, CA) using parametric and non-parametric unpaired t-tests. The results are expressed as the mean ± standard error.

Results

Muscle fiber injury

Muscle fiber injury in the WT group was significantly greater than the TLR4m samples (WT: 45.5±9 vs. TLR4m: 15.8±6 percent injured fibers, n=8/group, $P < .03$, Fig 1C) indicating that inactive TLR4 receptor signaling preserves muscle fiber integrity during IR. Representative photomicrographs of the reperfused skeletal muscle in TLR4m and WT are demonstrated in Fig 1, *A-B*, respectively. There were no differences in skeletal muscle morphology between non-ischemic sham operated WT and TLR4m mice (data not shown).

MPO immunostaining of reperfused skeletal muscle

Quantitative analysis of MPO immunostaining of reperfused skeletal muscle from WT and TLR4m mice showed significantly more MPO positive cells in the WT mice than in the TLR4m mice (WT: 245±28 and TLR4m: 53±17 MPO positive cells/hpf; n=8/group, $P < .0001$, Fig 2). These infiltrates were more prominent in the interstitial and perivascular regions of WT (Fig 2B) as compared to TLR4m mice (Fig 2A). The tissue sections of the contralateral hind limbs not subjected to ischemia or reperfusion showed no evidence of MPO positive immunostaining.

Expression of NETs in reperfused skeletal muscle

Regions demonstrating increased cell density that were positive for the MPO marker also revealed intense immunostaining for NETs (Fig 3). Detection of NETs was greater in the

WT group (Fig 3A) than the TLR4m group (Fig 3B), mirroring the level of neutrophil detection by MPO (Fig 2). NETs were found largely in the interstitial tissue, perivascular space and within microvascular thrombi. The amount of NETs immunostaining was significantly lower in the TLR4m sections and was undetectable in the control contralateral hind limb tissue sections (Fig 3C), providing evidence that the origin of these NETs is predominantly the neutrophils. To explore the possibility of using DNase as a potential therapeutic agent to degrade the NETs and to demonstrate the specificity of the antibody to detect NETs, WT tissue sections were immunostained for NETs following DNAse treatment. Immunofluorescent images revealed a marked decrease in the detection of NETs in the interstitial, perivascular and microvascular thrombi of the WT sections following DNase treatment (Fig 4).

Biochemical Characterization of Reperfused Skeletal Muscle

iNOS mRNA expression—TLR4m mice had significantly less iNOS expression than WT mice at 48 hours (n=5/group, $p<0.03$; Fig 5). This finding suggests that TLR4 modulates expression of iNOS in skeletal muscle during hind limb ischemia reperfusion injury.

ATP—TLR4m samples contained significantly higher levels of ATP compared to WT samples following IR (TLR4m: 2.1±0.4 vs. WT: 1.06±0.3 nmole/mg tissue, n=5/group. p=0.04, Fig 1D). This finding further suggests that in the absence of a functional TLR4, there are preserved levels of ATP consistent with decreased levels of muscle fiber injury as demonstrated by histology.

NF-κB activity and I κ B α expression—To estimate the level of NF-κB activation in the hind limb tissues of the WT and the TLR4m groups, nuclear extracts were assayed, revealing significant differences after 1 hour of reperfusion. The relative activation of the p65 subunit of NF-κB in the TLR4m group was significantly less than the wild type mice (TLR4m: 0.7342±0.05 vs. 1.145±0.11 AU, n=5/group, $P < .01$, Fig 6A). Thus, the acute activation of the transcription factor NF-κβ was markedly decreased in the TLR4m group compared to the wild type mice. However, at 48 hours reperfusion, the p65 NF-κβ activity was not significantly different between the two groups (TLR4m: 0.59±0.1 vs. 0.53±0.09 AU, $P < .69$, Fig 6A), suggesting that there may be an overlap between other cell receptor signaling pathways.

To further support the idea that the initial NF-κβ activation is markedly decreased in TLR4m mice, Western analysis was performed, which showed that the expression of the total IκBα subunit protein was significantly elevated in the hind limb muscle tissue of TLR4m compared to the WT group (28761±2282 IDV for TLR4m vs. 16934±1493 IDV for WT, $P < .003$, Fig 6, *B-C*) at 1 hour reperfusion. The quantity of phosphorylated IκBα protein, however, was not significantly different between the two groups (TLR4m: 9456±1987, WT: 4992±3382 IDV, $P < .06$, Fig 6, *B-C*).

PARP activity—TLR4m mice showed significant decrease in the poly ADP Ribose-modified proteins at 48 hours reperfusion compared to WT (3.86±0.87 for TLR4 vs. 8.1±1.6 IDV ratio, n=5/group. p=0.03, Fig 6, *D-E*). These data suggest that poly ADP ribose-modification of protein by PARP has been reduced in TLR4m, which implicate a link between PARP activity and TLR4 signaling pathway activity during skeletal muscle reperfusion injury.

Systemic Markers of Inflammation

CXC/KC (neutrophil chemokine), MCP-1 and VEGF levels in the serum samples of WT were compared to TLR4m samples. TLR4m serum samples showed decreased levels of the CXC cytokine KC compared to WT serum samples, however, this did not reach statistical difference (62±9 vs. 88±32pg/ml, respectively, p=NS; Fig 7A). In contrast, serum MCP-1 levels in the TLR4m group were significantly lower than the WT group (TLR4: 98±7 vs. WT; 257±18 pg/ml, n=6, P < .0002; Figure 7B). Additionally, TLR4m mice had significantly higher levels of the pro-angiogenic factor VEGF (TLR: 1272±377 vs. WT: 54±4 pg/ml, n=6, P < .015; Figure 7C). There were no detectable levels of KC, MCP-1 or VEGF in the serum of non ischemic WT and TLR4m mice. This data suggests that the WT group demonstrates a state of greater systemic inflammation than the TLR4m group. Moreover, the higher levels of VEGF detected in the TLR4m mice may result from the greater viable tissue remaining in the hind limb that is attempting to heal itself.

Discussion

These data are the first to implicate a role for TLR4 and NET's in skeletal muscle ischemia reperfusion injury. To date, the TLR family of proteins has been shown to play a pivotal role in mediating venous thrombosis and IR injury in the heart and brain.[16, 26, 34] In the studies in this report, TLR4m mice had a significant reduction in skeletal muscle fiber injury as compared to the WT mice (Fig 1). The decreased level of muscle fiber injury in the TLR4m group suggests that the ensuing intense inflammation in the WT group, likely plays a significant role in enhancing the level of tissue injury. It is unclear whether this increased injury is a direct result of NF-κB pathway activity, which is known to induce pro-inflammatory and pro-apoptotic genes,[2] or a secondary effect of the innate immune system resulting from leukocyte infiltration.

An analysis of the extent of inflammatory cell infiltration in reperfused skeletal muscle revealed that the decreased muscle fiber injury in the TLR4m group was associated with substantially less infiltration of MPO positive inflammatory cells (Fig 2). This observation of decreased MPO positive cell infiltration with decreased tissue injury is consistent with experiments geared towards neutrophil depletion in models of myocardial and small intestine IR.[15, 17] TLR4m mice were also found to have substantially less accumulation of NETs upon reperfusion. While NETs have been previously associated with cystic fibrosis,[19] venous thrombosis,[3] bacterial sepsis,[4] and cell death,[12] this is the first demonstration that NETs are present in reperfused skeletal muscle. Since the accumulation of leukocytes in the injured muscle tissue corresponded to marked detection of NETs, this strongly suggests that neutrophils are the most likely source of NETs in the injured muscle tissue; this is consistent with previous work demonstrating neutrophils as the dominant source of NETs production. [4, 5, 12, 36] NETs may further enhance the inflammatory response either directly by acting on TLRs or via histone mediated mechanisms. Extracellular histones have been shown to produce pathologic responses seen in sepsis such as cellular infiltration, endothelial cell dysfunction, thrombosis and organ failure. It was recently shown that TLR2 and TLR4 proteins mediate the sepsis-like response seen to extracellular histones and these histones were shown to activate platelets contributing to the development of microvascular thrombosis.[5, 20, 39, 40]

To determine whether DNase treatment, which is currently marketed as Pulmozyme used to treat NETs associated with cystic fibrosis, could destroy NETs in skeletal muscle, DNase was directly added to the surface of mounted slides of wild type reperfused skeletal muscle. Using this *ex vivo* technique, DNase completely depleted the NETs signal from detection. This finding will prompt future exploration of potential effectiveness of DNase therapy in an *in vivo* model of hind limb ischemia reperfusion.

The effects of the TLR4m on skeletal muscle ischemia reperfusion were not limited to the inflammatory cells. TLR4m mice had increased preservation of skeletal muscle high-energy phosphate levels (Fig 1D). This finding is also consistent with findings of ethyl pyruvate as a treatment for skeletal muscle IR. TLR4m mice had markedly decreased levels of iNOS mRNA expression, which is also consistent with decreased activation of macrophages in other models of inflammation. [23, 29] The decreased activation of the NF-κβ pathway indicates that the TLR4 receptor MyD88-dependent pathway likely modulates the NF-κβ pathway activity during reperfusion injury. As expected, the decrease in NF-κβ expression was associated with increased IkBα expression, which suggests that the decrease in NF-κB is not a nonspecific event. Further evidence to suggest the specificity of decreased cellular stress in the TLR4m mice subjected to hind limb IR was the observed decrease in PARP activation. A previous report from our lab using pharmacologic interventions in a clinically relevant post hoc scenario showed only a transient decrease in PARP activity at 7 hours reperfusion,[6] whereas in this report, a significant decrease in PARP activity was observed even at 48 hours reperfusion.

TLR4m mice had substantially decreased systemic levels of the proinflammatory cytokine, MCP-1, but not KC. MCP-1 deficiency has been shown to alter skeletal muscle healing[1], and thus it is not clear that its reduction in the TLR4m is beneficial. It is possible that MCP-1, like IL-6 may have pro and anti-inflammatory properties at different times in a physiologic process. In contrast to decreased MCP-1, circulating levels of VEGF levels were increased in the TLR4m group. This may mean that inhibiting the activity of TLR4 may potentiate post-ischemic angiogenic pathways.

There are several limitations of our study. The use of pharmacologic inhibitors of TLR4 or its downstream intracellular signaling proteins would provide more information on the potential for clinically targeting TLR4.[22, 27, 38] Furthermore, it is not clear that the presence of NETs is deleterious or cytoprotective. This issue may be further studied by intravenous or intraperitoneal nuclease treatment, such as DNase-1, to degrade NETs. IR injury in MPO or NADPH oxidase knockout mice,[14, 24] which are known to be deficient in the production of NETs, may also help demonstrate the potential role NETs may play in IR injury.

In conclusion, we show that IR injury in the murine hind limb is modulated by a functional TLR4 suggesting that its inhibition prior to interventions in acute limb ischemia may be a potential strategy to minimize IR injury in patients. This increased muscle fiber injury is associated with marked infiltration of neutrophils and marked detection of NETs in the injured tissue. It is possible that NETs further intensifies the hind limb muscle injury given the known deleterious effects of histones. While *ex vivo* nuclease pretreatment of the hind limb muscle tissue sections diminishes the level of NETs detection, it remains to be shown whether *in vivo* nuclease treatment will ameliorate IR injury in the hind limb muscle tissue.

Acknowledgments

MTW is the Isenberg Scholar In Academic Surgery at the Massachusetts General Hospital. This study was supported by NIH grant RO1 AR055843 (MTW), Pacific Vascular Research Foundation, the Department of Surgery, Division of Vascular and Enbdovascular Surgery (The Rosenberg Fund). RO is funded by the American College of Phlebology and the Department of Radiology, Division of Vascular Imaging and Intervention.

References

1. Abbruzzese TA, Albadawi H, Kang J, Patel VI, Yoo JH, Lamuraglia GM, et al. Enoxaparin does not ameliorate limb ischemia-reperfusion injury. J Surg Res. 2008; 147:260–266. [PubMed: 18498878]
2. Akira S, Takeda K. Toll-like receptor signalling. Nature reviews Immunology. 2004; 4:499–511.

3. Brill A, Fuchs TA, Savchenko AS, Thomas GM, Martinod K, De Meyer SF, et al. Neutrophil extracellular traps promote deep vein thrombosis in mice. J Thromb Haemost. 2012; 10:136–144. [PubMed: 22044575]
4. Brinkmann V, Reichard U, Goosmann C, Fauler B, Uhlemann Y, Weiss DS, et al. Neutrophil extracellular traps kill bacteria. Science. 2004; 303:1532–1535. [PubMed: 15001782]
5. Clark SR, Ma AC, Tavener SA, McDonald B, Goodarzi Z, Kelly MM, et al. Platelet TLR4 activates neutrophil extracellular traps to ensnare bacteria in septic blood. Nat Med. 2007; 13:463–469. [PubMed: 17384648]
6. Crawford RS, Albadawi H, Atkins MD, Jones JE, Yoo HJ, Conrad MF, et al. Postischemic poly (ADP-ribose) polymerase (PARP) inhibition reduces ischemia reperfusion injury in a hind-limb ischemia model. Surgery. 2010; 148:110–118. [PubMed: 20132957]
7. Crawford RS, Albadawi H, Atkins MD, Jones JJ, Conrad MF, Austen WG Jr, et al. Postischemic treatment with ethyl pyruvate prevents adenosine triphosphate depletion, ameliorates inflammation, and decreases thrombosis in a murine model of hind-limb ischemia and reperfusion. J Trauma. 2011; 70:103–110. [PubMed: 21217488]
8. Crawford RS, Hashmi FF, Jones JE, Albadawi H, McCormack M, Eberlin K, et al. A novel model of acute murine hindlimb ischemia. Am J Physiol Heart Circ Physiol. 2007; 292:H830–H837. [PubMed: 17012358]
9. Doring Y, Soehnlein O, Drechsler M, Shagdarsuren E, Chaudhari SM, Meiler S, et al. Hematopoietic interferon regulatory factor 8-deficiency accelerates atherosclerosis in mice. Arterioscler Thromb Vasc Biol. 2012; 32:1613–1623. [PubMed: 22556330]
10. Dubois AV, Gauthier A, Brea D, Varaigne F, Diot P, Gauthier F, et al. Influence of DNA on the activities and inhibition of neutrophil serine proteases in cystic fibrosis sputum. Am J Respir Cell Mol Biol. 2012; 47:80–86. [PubMed: 22343221]
11. Fan J, Kapus A, Marsden PA, Li YH, Oreopoulos G, Marshall JC, et al. Regulation of Toll-like receptor 4 expression in the lung following hemorrhagic shock and lipopolysaccharide. J Immunol. 2002; 168:5252–5259. [PubMed: 11994482]
12. Fuchs TA, Abed U, Goosmann C, Hurwitz R, Schulze I, Wahn V, et al. Novel cell death program leads to neutrophil extracellular traps. J Cell Biol. 2007; 176:231–241. [PubMed: 17210947]
13. Fuchs TA, Brill A, Duerschmied D, Schatzberg D, Monestier M, Myers DD Jr, et al. Extracellular DNA traps promote thrombosis. Proc Natl Acad Sci U S A. 2010; 107:15880–15885. [PubMed: 20798043]
14. Gao XP, Standiford TJ, Rahman A, Newstead M, Holland SM, Dinauer MC, et al. Role of NADPH oxidase in the mechanism of lung neutrophil sequestration and microvessel injury induced by Gram-negative sepsis: studies in p47phox-/- and gp91phox-/- mice. J Immunol. 2002; 168:3974–3982. [PubMed: 11937554]
15. Granfeldt A, Jiang R, Wang NP, Mykytenko J, Eldaif S, Deneve J, et al. Neutrophil inhibition contributes to cardioprotection by postconditioning. Acta Anaesthesiol Scand. 2012; 56:48–56. [PubMed: 22103673]
16. Henke PK, Mitsuya M, Luke CE, Elfline MA, Baldwin JF, Deatrick KB, et al. Tolllike receptor 9 signaling is critical for early experimental deep vein thrombosis resolution. Arterioscler Thromb Vasc Biol. 2011; 31:43–49. [PubMed: 20966396]
17. Liu Y, Kalogeris T, Wang M, Zuidema MY, Wang Q, Dai H, et al. Hydrogen sulfide preconditioning or neutrophil depletion attenuates ischemia-reperfusion-induced mitochondrial dysfunction in rat small intestine. Am J Physiol Gastrointest Liver Physiol. 2012; 302:G44–G54. [PubMed: 21921289]
18. Losman MJ, Fasy TM, Novick KE, Monestier M. Monoclonal autoantibodies to subnucleosomes from a MRL/Mp(−)+/+ mouse. Oligoclonality of the antibody response and recognition of a determinant composed of histones H2A, H2B, and DNA. J Immunol. 1992; 148:1561–1569. [PubMed: 1371530]
19. Marcos V, Zhou Z, Yildirim AO, Bohla A, Hector A, Vitkov L, et al. CXCR2 mediates NADPH oxidase-independent neutrophil extracellular trap formation in cystic fibrosis airway inflammation. Nat Med. 2010; 16:1018–1023. [PubMed: 20818377]

20. Massberg S, Grahl L, von Bruehl ML, Manukyan D, Pfeiler S, Goosmann C, et al. Reciprocal coupling of coagulation and innate immunity via neutrophil serine proteases. Nat Med. 2010; 16:887–896. [PubMed: 20676107]
21. McCormack MC, Kwon E, Eberlin KR, Randolph M, Friend DS, Thomas AC, et al. Development of reproducible histologic injury severity scores: skeletal muscle reperfusion injury. Surgery. 2008; 143:126–133. [PubMed: 18154940]
22. Mullarkey M, Rose JR, Bristol J, Kawata T, Kimura A, Kobayashi S, et al. Inhibition of endotoxin response by e5564, a novel Toll-like receptor 4-directed endotoxin antagonist. J Pharmacol Exp Ther. 2003; 304:1093–1102. [PubMed: 12604686]
23. Muthupalani S, Ge Z, Feng Y, Rickman B, Mobley M, McCabe A, et al. Systemic macrophage depletion inhibits Helicobacter bilis-induced proinflammatory cytokine-mediated typhlocolitis and impairs bacterial colonization dynamics in a BALB/c Rag2−/−mouse model of inflammatory bowel disease. Infect Immun. 2012; 80:4388–4397. [PubMed: 23027534]
24. Nguyen HX, Lusis AJ, Tidball JG. Null mutation of myeloperoxidase in mice prevents mechanical activation of neutrophil lysis of muscle cell membranes in vitro and in vivo. J Physiol. 2005; 565:403–413. [PubMed: 15790660]
25. Oklu R, Albadawi H, Watkins MT, Monestier M, Sillesen M, Wicky S. Detection of extracellular genomic DNA scaffold in human thrombus: implications for the use of deoxyribonuclease enzymes in thrombolysis. J Vasc Interv Radiol. 2012; 23:712–718. [PubMed: 22525027]
26. Oyama J, Blais C Jr, Liu X, Pu M, Kobzik L, Kelly RA, et al. Reduced myocardial ischemia-reperfusion injury in toll-like receptor 4-deficient mice. Circulation. 2004; 109:784–789. [PubMed: 14970116]
27. Parker LC, Whyte MK, Vogel SN, Dower SK, Sabroe I. Toll-like receptor (TLR)2 and TLR4 agonists regulate CCR expression in human monocytic cells. J Immunol. 2004; 172:4977–4986. [PubMed: 15067079]
28. Poltorak A, He X, Smirnova I, Liu MY, Van Huffel C, Du X, et al. Defective LPS signaling in C3H/HeJ and C57BL/10ScCr mice: mutations in Tlr4 gene. Science. 1998; 282:2085–2088. [PubMed: 9851930]
29. Riquelme P, Tomiuk S, Kammler A, Fandrich F, Schlitt HJ, Geissler EK, et al. IFN-gamma-induced iNOS Expression in Mouse Regulatory Macrophages Prolongs Allograft Survival in Fully Immunocompetent Recipients. Mol Ther. 2012
30. Sappington PL, Cruz RJ Jr, Harada T, Yang R, Han Y, Englert JA, et al. The ethyl pyruvate analogues, diethyl oxaloproprionate, 2-acetamidoacrylate, and methyl-2-acetamidoacrylate, exhibit anti-inflammatory properties in vivo and/or in vitro. Biochem Pharmacol. 2005; 70:1579–1592. [PubMed: 16226725]
31. Schreiber A, Pham CT, Hu Y, Schneider W, Luft FC, Kettritz R. Neutrophil serine proteases promote IL-1beta generation and injury in necrotizing crescentic glomerulonephritis. J Am Soc Nephrol. 2012; 23:470–482. [PubMed: 22241891]
32. Shen XD, Gao F, Ke B, Zhai Y, Lassman CR, Tsuchihashi S, et al. Inflammatory responses in a new mouse model of prolonged hepatic cold ischemia followed by arterialized orthotopic liver transplantation. Liver Transpl. 2005; 11:1273–1281. [PubMed: 16184555]
33. Shen XD, Ke B, Zhai Y, Gao F, Busuttil RW, Cheng G, et al. Toll-like receptor and heme oxygenase-1 signaling in hepatic ischemia/reperfusion injury. Am J Transplant. 2005; 5:1793–1800. [PubMed: 15996225]
34. Tang SC, Arumugam TV, Xu X, Cheng A, Mughal MR, Jo DG, et al. Pivotal role for neuronal Toll-like receptors in ischemic brain injury and functional deficits. Proc Natl Acad Sci U S A. 2007; 104:13798–13803. [PubMed: 17693552]
35. Tsung A, Hoffman RA, Izuishi K, Critchlow ND, Nakao A, Chan MH, et al. Hepatic ischemia/reperfusion injury involves functional TLR4 signaling in nonparenchymal cells. Journal of immunology. 2005; 175:7661–7668.
36. Wang Y, Li M, Stadler S, Correll S, Li P, Wang D, et al. Histone hypercitrullination mediates chromatin decondensation and neutrophil extracellular trap formation. J Cell Biol. 2009; 184:205–213. [PubMed: 19153223]

37. Wu H, Chen G, Wyburn KR, Yin J, Bertolino P, Eris JM, et al. TLR4 activation mediates kidney ischemia/reperfusion injury. J Clin Invest. 2007; 117:2847–2859. [PubMed: 17853945]

38. Wu Y, Lousberg EL, Moldenhauer LM, Hayball JD, Coller JK, Rice KC, et al. Inhibiting the TLR4-MyD88 signalling cascade by genetic or pharmacological strategies reduces acute alcohol-induced sedation and motor impairment in mice. Br J Pharmacol. 2012; 165:1319–1329. [PubMed: 21955045]

39. Xu J, Zhang X, Monestier M, Esmon NL, Esmon CT. Extracellular histones are mediators of death through TLR2 and TLR4 in mouse fatal liver injury. J Immunol. 2011; 187:2626–2631. [PubMed: 21784973]

40. Xu J, Zhang X, Pelayo R, Monestier M, Ammollo CT, Semeraro F, et al. Extracellular histones are major mediators of death in sepsis. Nat Med. 2009; 15:1318–1321. [PubMed: 19855397]

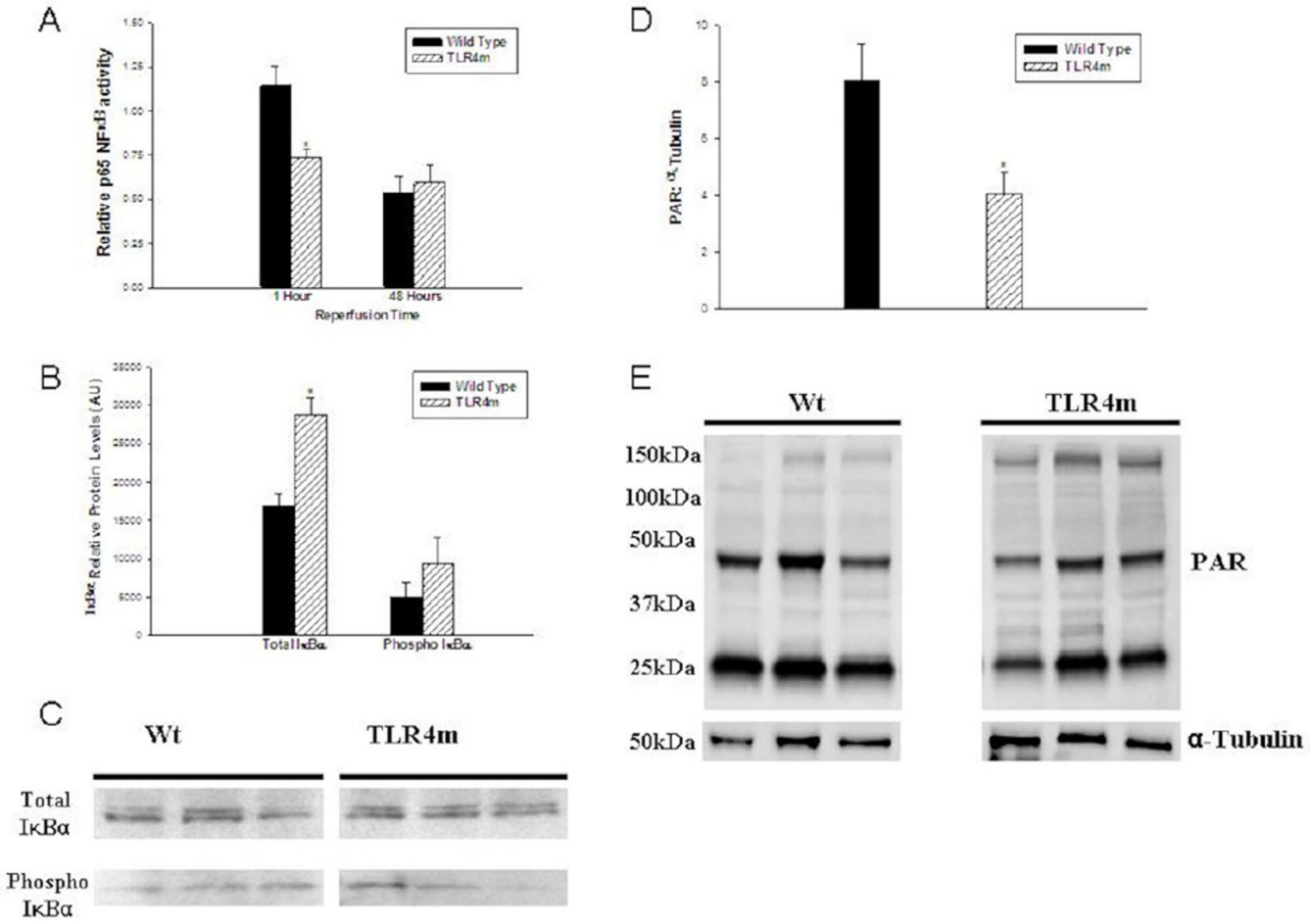

Figure 1.

Hemotoxylin and eosin staining of the murine hind limb muscle tissue sections following 1.5 hours of ischemia and 48 hours of reperfusion; representative images are shown. (a) TLR4m tissue sections show relatively preserved muscle fibers with scattered fiber injury, indicated by the black arrows, and tissue edema. (b) Wild type tissue sections show significantly greater muscle fiber injury; black arrows indicate examples of injured fibers. (c) There was significantly greater muscle fiber injury in the wild type hind limb muscle groups, gastrocnemius and anterior tibialis, compared to the TLR4m tissues (*$p<0.05$, **$p<0.01$, respectively). Increased muscle fiber injury in wild type mice (c) was consistent with significantly decreased ATP levels (d) compared to the less injured, TLR4m group showing much higher ATP levels (*$p<0.04$). Black bar in (a) and (b) represents 100 microns.

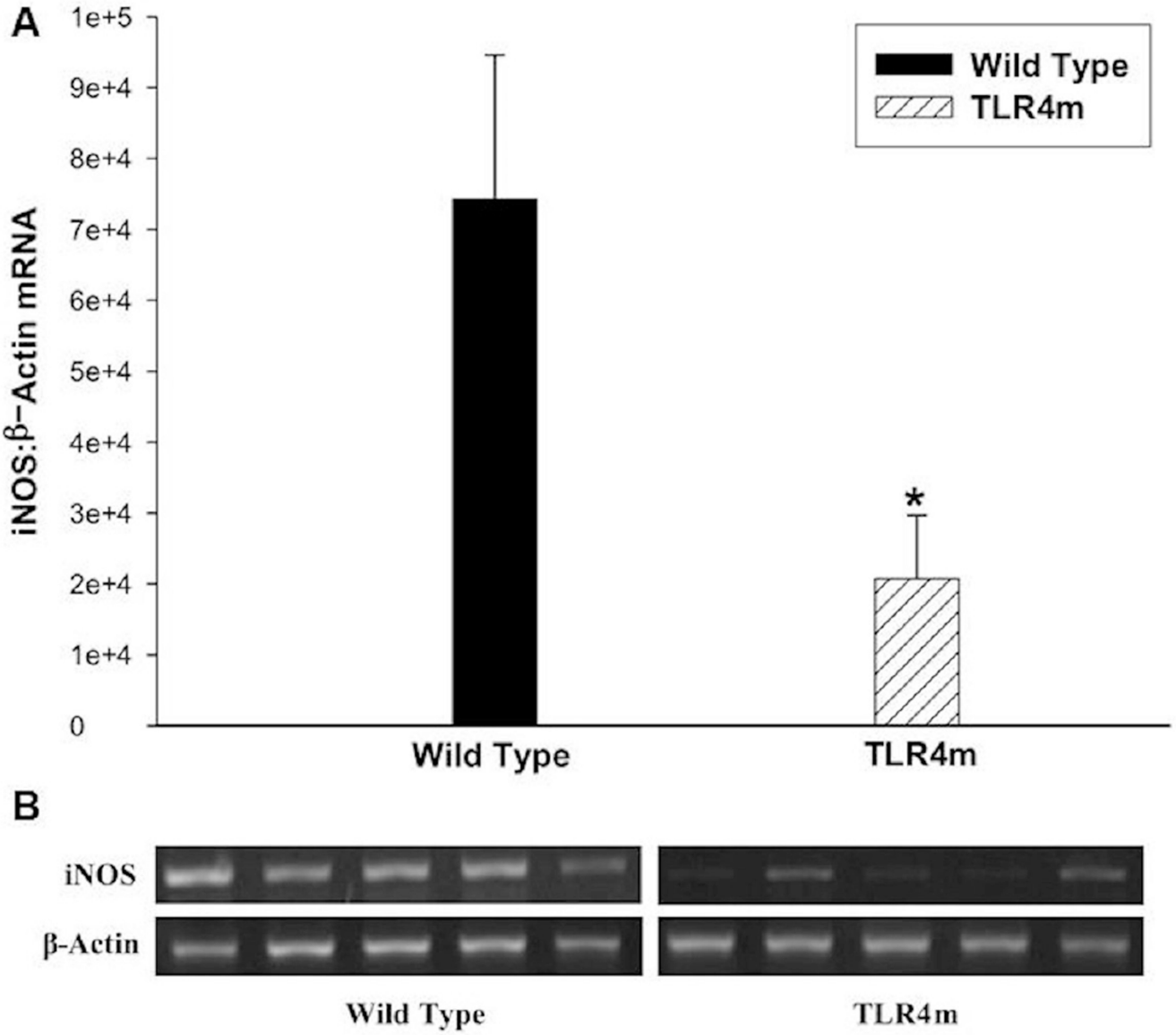

Figure 2.

Immunohistochemical detection of MPO in murine hind limb muscle tissue sections following 1.5 hours of ischemia and 48 hours of reperfusion; representative images are shown. (a) TLR4m mice showed significantly less, brown immunostained, MPO positive cells in muscle tissue than the wild type group (b). Black arrows indicate examples of MPO containing cells. (c) There was more than five-fold greater MPO immunostained cells within the tissue sections of wild type mice compared to the TLR4m mice (*$p < .0001$). Black bar in (a) and (b) represents 100 microns.

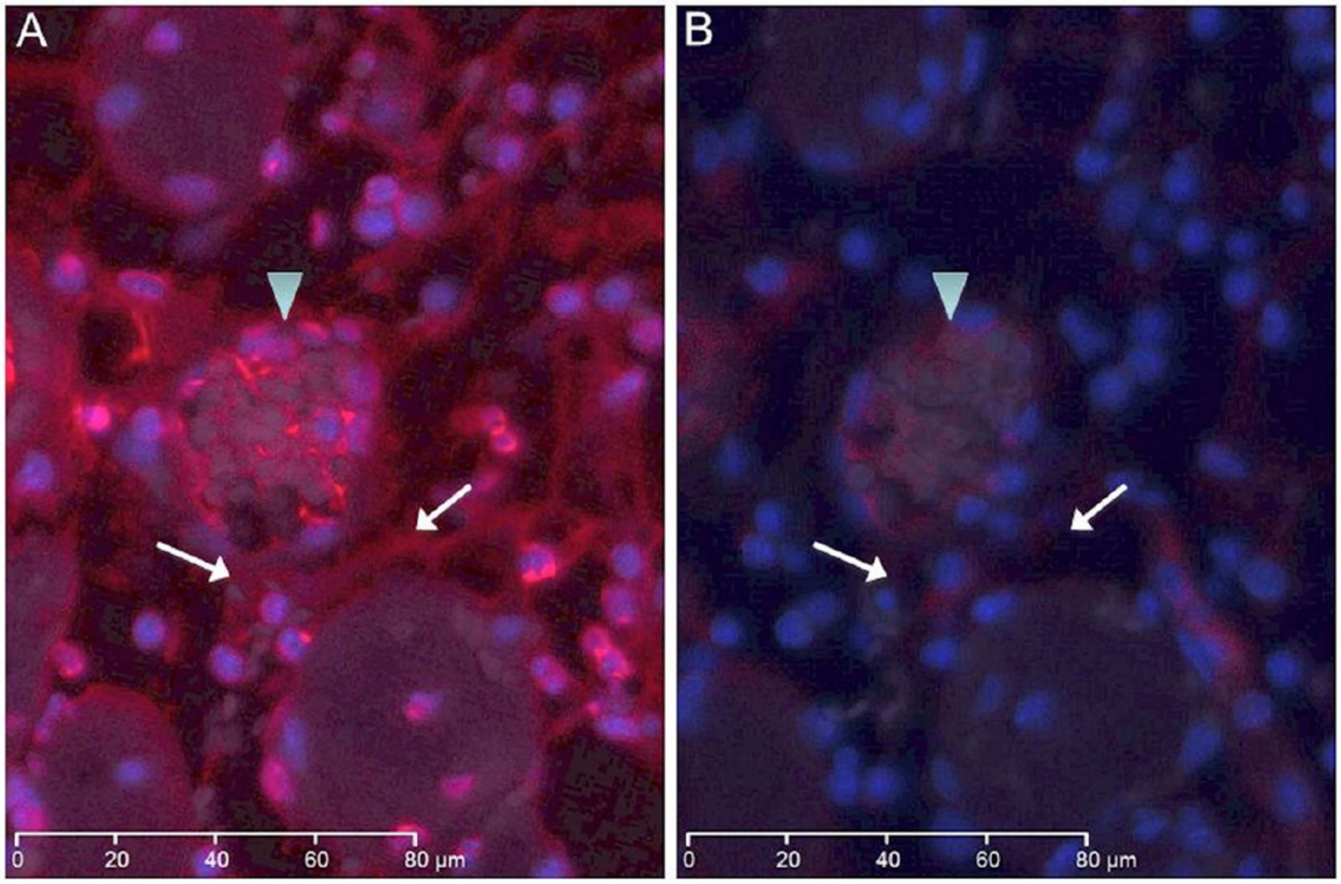

Figure 3.

Immunostaining for NETs in murine hind limb IR injury using the monoclonal anti-histone H2A/H2B/DNA complex antibody; representative images are shown. (a) WT tissue sections show extensive immunostaining for NETs, indicated by brown color, in interstitial tissue (arrowhead) and in thrombi (arrow) within vessels. There is increased cellular density in regions of intense NETS detection. (b) TLR4m tissue section showing minimal if any interstitial (arrowhead) and intravascular NETs (arrow) immunostaining. (c) Contralateral hind limb muscle fibers are normal with positive immunostaining only in the nuclei of muscle fibers. (d) Negative control. Black bar in each image represents 200 microns.

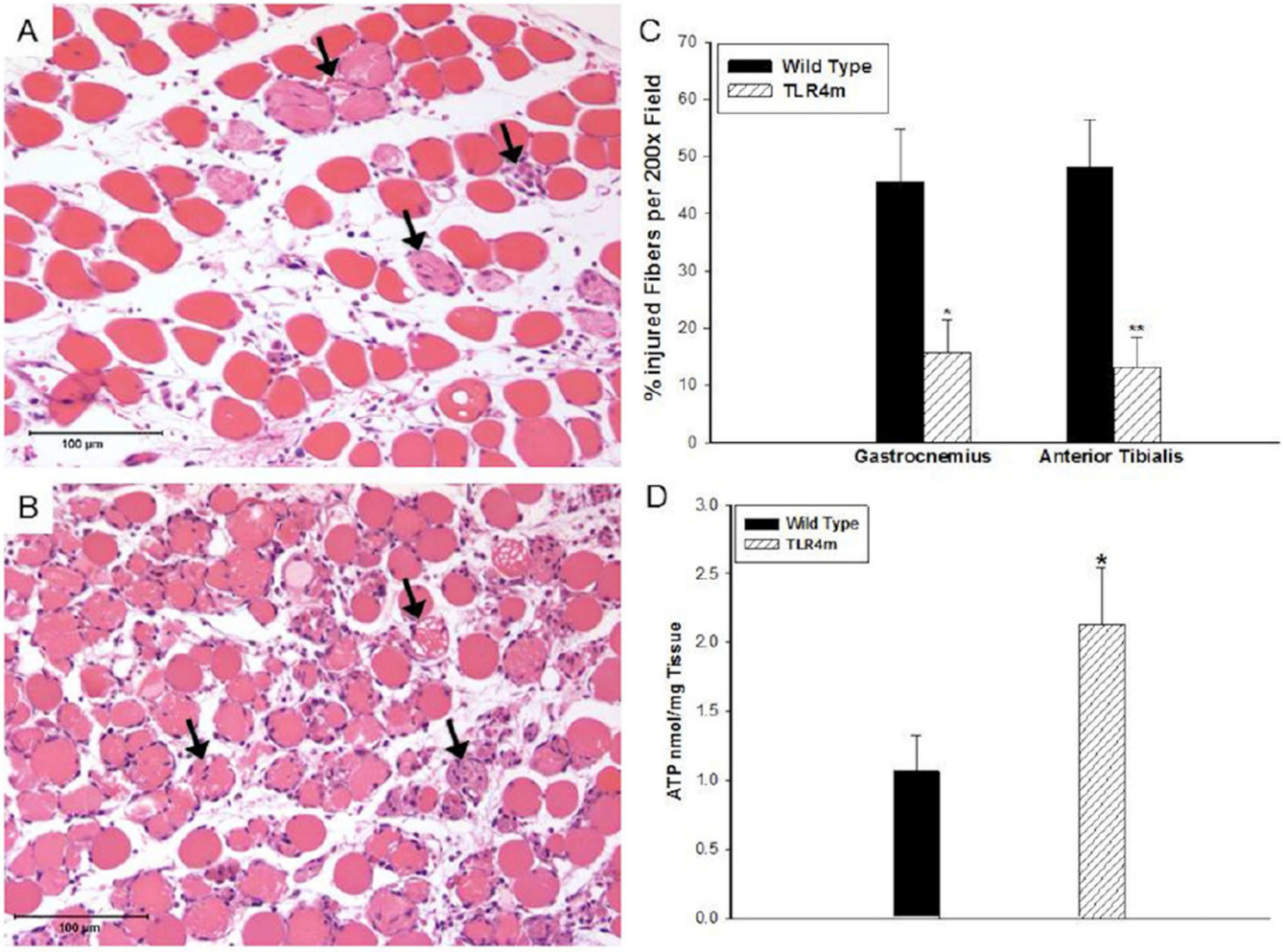

Figure 4.

Immunofluorescent images show NETs in red and nuclear DNA in blue in WT tissue section with and without DNAse treatment. (a) WT tissue section demonstrates detection of NETs in a thrombosed vein (arrowhead) and in the interstitium (arrows). (b) Adjacent tissue section was immunostained for NETs following an initial incubation with DNase enzyme. The section shows significant decrease in NETs signal suggesting that nuclease pretreatment markedly reduced the level of antigen available for detection. The white bar in each image represents 80 microns.

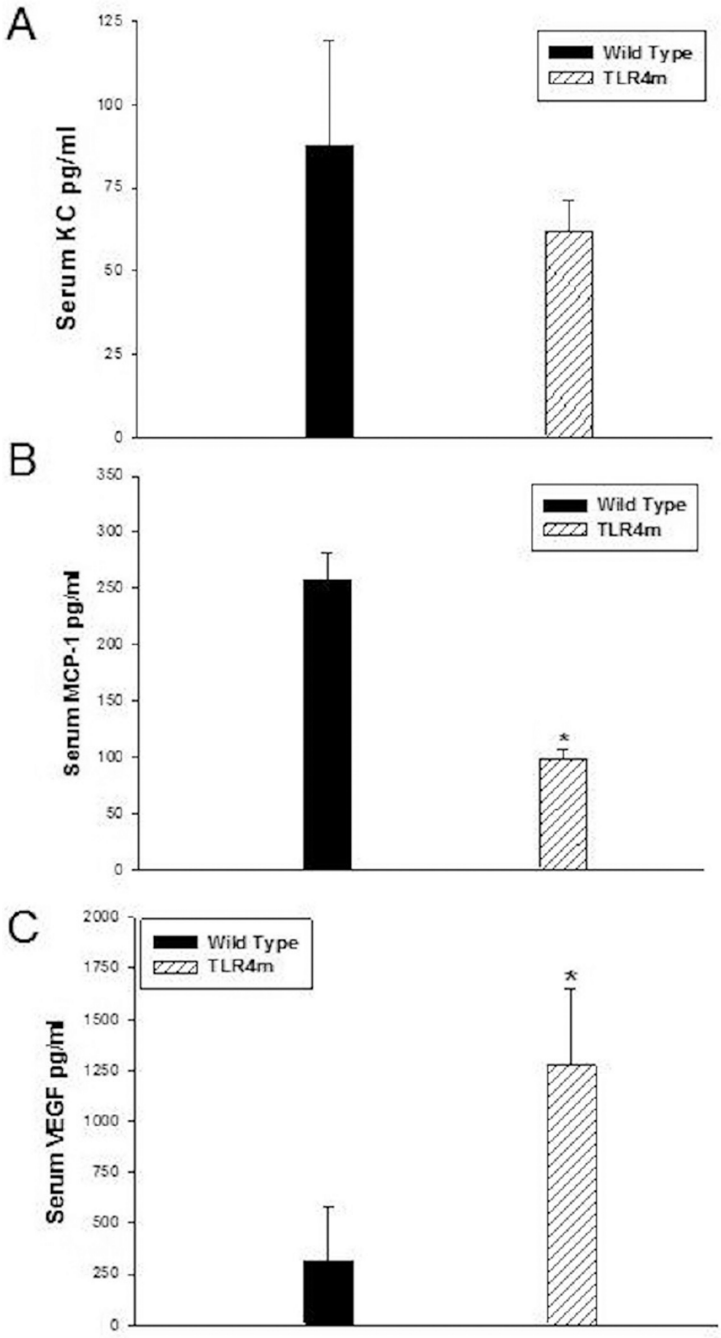

Figure 5.

iNOS mRNA expression in IR injured murine skeletal muscles using semiquantitative RT-PCR. (a) TLR4m mice had significantly less iNOS mRNA expression than wild type mice (*$p<0.03$) normalized to β-actin. (b) A representative image of the agarose gel showing the iNOS and β-actin bands from the two groups of tissue samples.

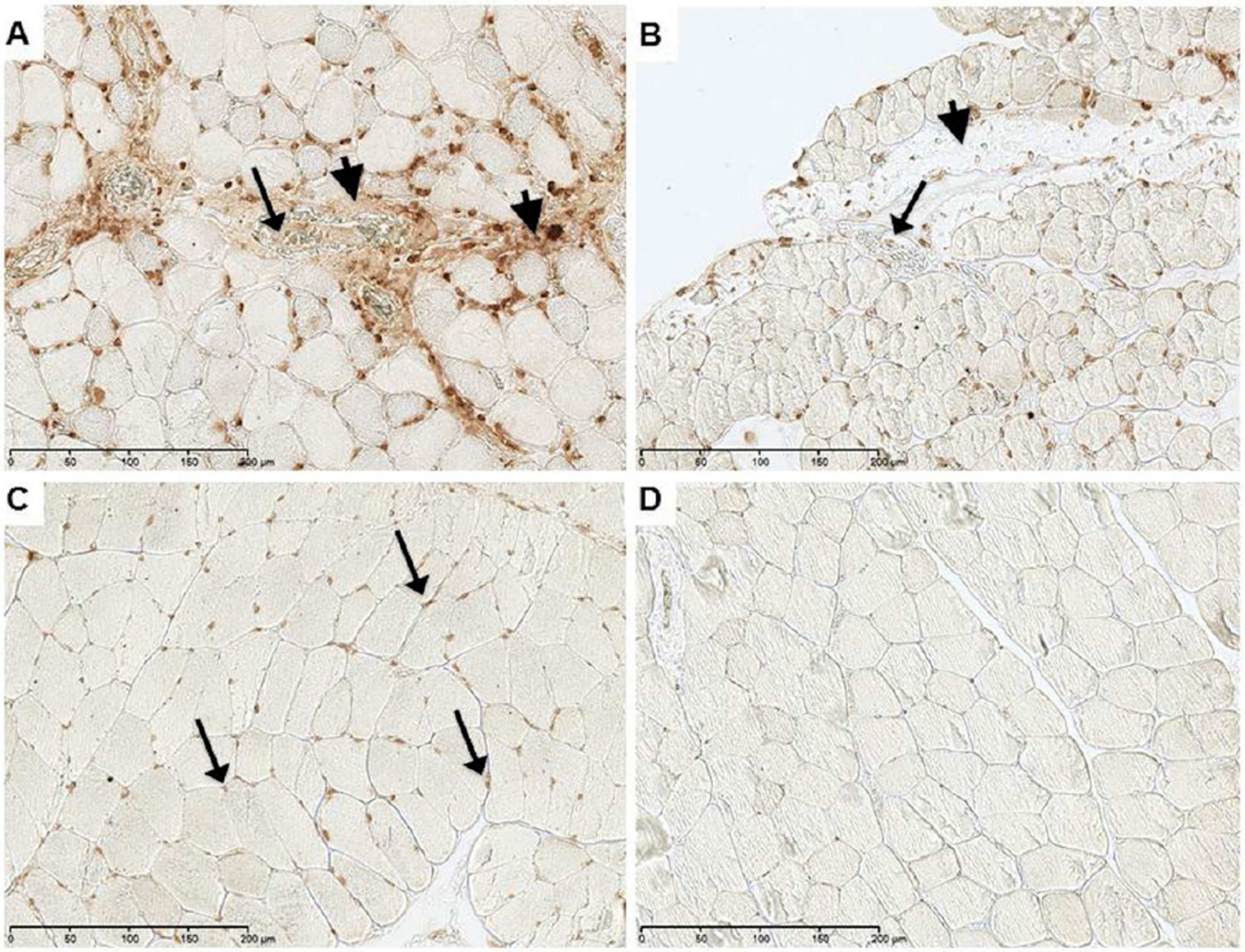

Figure 6.

(a) Relative detection of p65 NF-κβ activity using an ELISA assay in murine hind limb muscle tissue following IR. TLR4m mice had less p65 NF-κβ activity compared to WT mice following 1.5 hours of ischemia and one hour of reperfusion (*p=0.0025). By 48 hours there was no difference in p65 NF- κβ activity detected between the two groups. (b) IκBα protein levels were quantitated using a Western blot analysis following 1.5 hours of ischemia and 1 hour of reperfusion. TLR4m mice had significantly greater levels of total IκBα in reperfused skeletal muscle compared to WT mice (*p<0.01). In contrast there was no significant difference in the Ser32-phosphorylation of IκBα. (c) Representative Western blot analysis of three WT and three TLR4m derived muscle tissues. (d) TLR4m mice showed significant decrease in the poly ADP ribose-modified proteins at 48 hours reperfusion compared to WT (*p=0.032). (e) Representative Western blot image of the detected poly ADP ribose-modified proteins in three WT and three TLR4m skeletal muscle tissues.

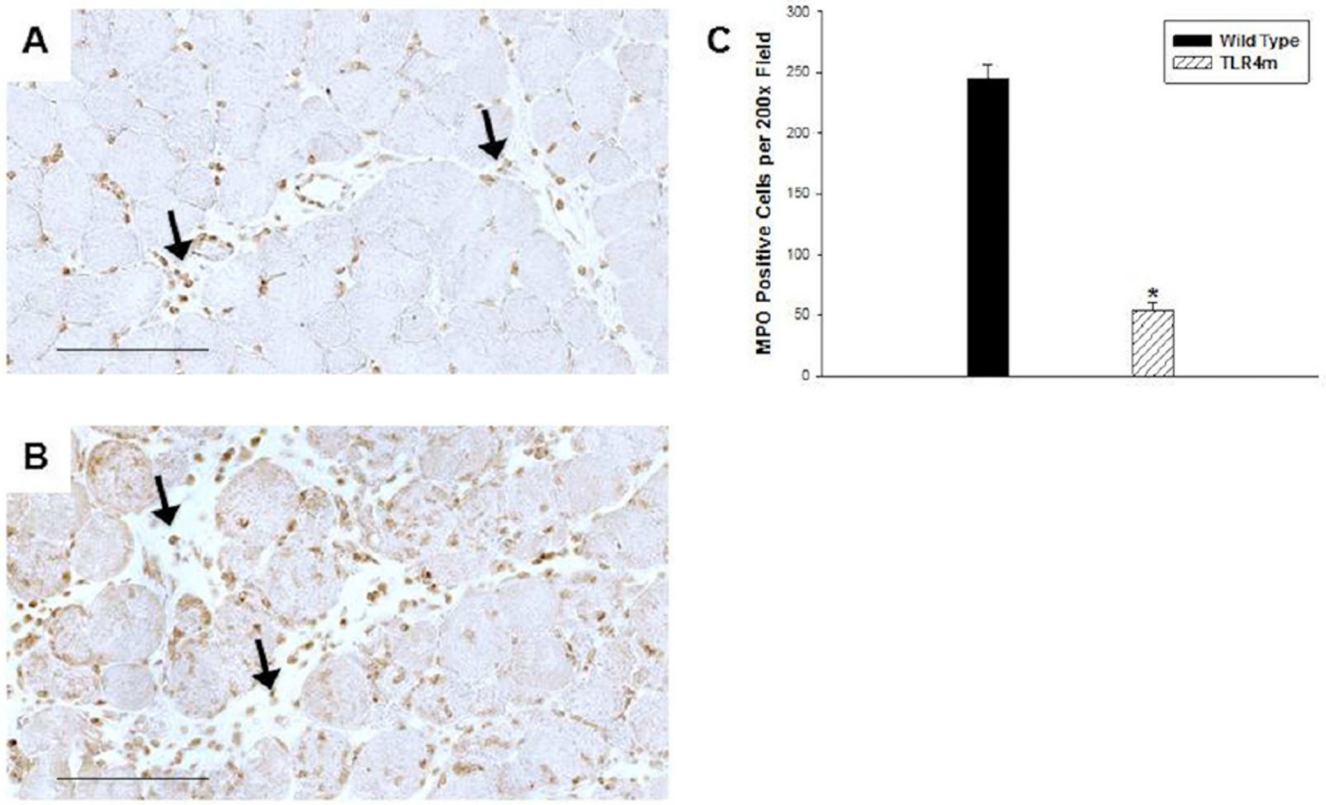

Figure 7.

Quantitation of systemic markers of inflammation, KC, MCP-1 and VEGF. (a) TLR4m and WT mice had similar levels of the CXC cytokine KC. In contrast, (b) serum MCP-1 levels in TLR4m mice were significantly lower than WT mice following 48 hours of reperfusion (*p=0.0002). (c) TLR4m mice also demonstrated significantly higher level of the pro-angiogenic factor VEGF (*p=0.015).